The Egyptian Journal of Radiology and Nuclear Medicine (2011) **42**, 289–295

Egyptian Society of Radiology and Nuclear Medicine

The Egyptian Journal of Radiology and Nuclear Medicine

www.elsevier.com/locate/ejrnm
www.sciencedirect.com

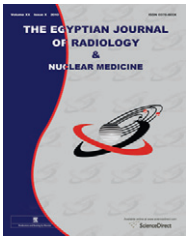

ORIGINAL ARTICLE

Tetralogy of Fallot: Imaging of common and uncommon associations by multidetector CT

Rania H. Zakaria, Nadine R. Barsoum *, Ramy E. Asaad, Ayman A. El-Basmy, Amr O. Azab

Radiology Department, Faculty of Medicine, Cairo University, Alfa Scan Radiology Center, 1 Hegaz Square, Mohandeseen, Cairo 11513, Egypt

Received 16 July 2011; accepted 31 July 2011
Available online 27 August 2011

KEYWORDS

Pediatric cardiology;
Tetralogy of Fallot;
Multidetector CT;
Cardiac radiology

Abstract *Purpose:* To demonstrate the superior role of multidetector computed tomography (MDCT) in delineation of the extracardiac vascular abnormalities including the pulmonary arterial tree, major aortopulmonary collateral arteries (MAPCAs), patent ductus arteriosus (PDA), and also the detection of the common and uncommon findings in Fallot Tetralogy cases for proper pre-surgical evaluation.

Material and methods: A retrospective study of all multidetector CT images acquired to evaluate suspected cases of Tetralogy of Fallot sent by their respective referring physicians between April 2009 and August 2010. A total of 23 cases were included in this study. MDCT protocol, image analysis and calculations used in the diagnosis are explained in detail.

Results: Detailed explanation of the MDCT imaging findings in the 23 cases with Tetralogy of Fallot, as well as the common and uncommon associations of the disease, namely pulmonary atresia, MAPCAs, PDAs, atrial septal defects (ASDs), right sided aortic arch, and a few less common associations.

* Corresponding author. Address: 3 Hussein El Memar Street, P.O. Box 91, Antikhana, Cairo 11513, Egypt. Tel.: +20 123080177; fax: +20 225758932.
E-mail address: nadinebarsoum@gmail.com (N.R. Barsoum).

Peer review under responsibility of Egyptian Society of Radiology and Nuclear Medicine.
doi:10.1016/j.ejrnm.2011.07.003

ELSEVIER **Production and hosting by Elsevier**

Conclusion: A customized approach to MDCT imaging improves the diagnostic accuracy and reduces unneeded prolongation of the study and sedation times. A careful preoperative perceptive of the complex cardiovascular anatomy in patients with Tetralogy of Fallot aids in exposing the patient to a directed and prepared surgical approach.

1. Introduction

The Tetralogy of Fallot was first described by Louis Arthur Etienne Fallot in 1888 as "La Maladie Bleue" (1). It is a clinical condition created by a group of anatomical malformations with fundamental features consisting of an interventricular communication, also known as ventricular septal defect, biventricular connection of the aortic root, overriding the muscular ventricular septum, obstruction of the right ventricular outflow tract, and right ventricular hypertrophy (2). The manifestations and management of the disease are dependent on the severity of each component.

The combination of these malformations occurs in 3 of every 10,000 live births, and accounts for 7–11% of all congenital heart disease (CHD) (3,4).

Common associations of Fallot's Tetralogy are pulmonary artery atresia (varying from mild hypoplasia to complete absence of the main pulmonary artery or the non-confluence of its branches), right-sided aortic arch in 25% of cases, atrial septal defect (ASD) in 10% of cases (so called pentalogy of Fallot) and coronary artery abnormalities in 10% of cases. Other less common associations include persistent left superior vena cava (SVC) and aberrant right subclavian artery. Rarely, tracheoesophageal fistula, rib anomalies, and scoliosis may be encountered (5–7).

At present, surgical correction is performed by closure of the VSD and relief of right ventricular outflow obstruction when patients are young (7–9). So in order to plan an effective management of the disease, the surgeon needs the best perception of the malformation.

Although echocardiography and angiography are the traditional imaging modalities in patients with CHD, magnetic resonance (MR) imaging and multidetector computed tomography (MDCT) are valuable noninvasive options. They are useful in demonstrating the complex cardiovascular morphology of Fallot's Tetralogy, especially the extracardiac associations as well as the pulmonary artery anatomy and aortopulmonary collateral vessels (10).

The development of 64-section MDCT, with its high scanning speed, superior spatial resolution, and improved capabilities for concurrent assessment of cardiovascular structures and lung parenchyma, has improved its application for evaluation of patients with CHD even in small infants (11). When combined with electrocardiographic (ECG) gating, CT images perfectly define the moving cardiac and paracardiac structures and permits evaluation of associated coronary artery anomalies (12,13). Multiplanar reformation is easily obtainable with the new advanced software thus reducing the prior disadvantage of CT image acquisition being solely in the transaxial plane (10).

The purpose of this study is to demonstrate the superior role of MSCT in delineation of the extracardiac vascular abnormalities including the pulmonary arterial tree, MAPCAs, and patent ductus arteriosus (PDA), and also the detection of the common and uncommon findings in Fallot Tetralogy cases for proper pre-surgical evaluation.

2. Patients and methods

We retrospectively reviewed all multidetector CT images acquired to evaluate suspected cases of Tetralogy of Fallot sent by their respective referring physicians between April 2008 and August 2009 within a single institution. This yielded a total of 25 cases who were examined by MDCT. The findings in these patients had been previewed, hence two cases were immediately discarded from the study, as they were not diagnosed as Tetralogy of Fallot by MDCT imaging and the preliminary clinical diagnosis was proven to be false. The patient population consisted of 8 males and 15 female patients with a mean age of 2.3 ± 3.6 years (range one day to 12 years). A written consent was gathered retrospectively from the parents of all the patients included in the study. The MDCT results were correlated with the results of echocardiography (n = 23 cases). CT scans were obtained with a 64-section CT scanner (Toshiba Aquillion One). The patients were divided into four main groups: those with classic Tetralogy of Fallot with no associations (n = 2), those with common associations (n = 5), those with uncommon associations (n = 5) and those with a combination of common and uncommon associations (n = 11).

2.1. MDCT imaging protocol

Data acquisition was performed in a craniocaudal direction from the level of the thoracic inlet down to the diaphragm. The scanning parameters include detector collimation of 32–0.6 mm, section collimation of 64–0.6 mm by means of a z-flying focal spot, gantry rotation time of 330 ms, pitch of 0.2 and tube potential of 120 kVp.

ECG-controlled tube current modulation (ECG pulsing) was applied with a nominal tube current during diastole (600 mA s) and a reduced tube current during systole (120 mA s). The use of this technique leads to a considerable reduction in radiation dose. However this technique was not feasible in patients with high heart rates (>200 beats per minute). Thus, ECG-gating CT in children was performed only in the presence of specific indications that outweigh the potential risk of radiation exposure.

Contrast enhancement was achieved by non-ionic contrast agent (Ultravist 300 [iopromide], Schering, Berlin, Germany) calculated according to the patient weight, with a maximum dose of 2 ml/kg (much lower than that needed in catheterization where the dose may reach up to 5 ml/kg), injected at 2 ml/s, pressure 100 through an 22-gauge catheter into peripheral vein. Scanning initiation was triggered by identification of a density of 150 H in the ascending aorta. Images were reconstructed at the optimum phase of the R–R interval with the

least motion artifacts (0% was optimum in most patients, sometimes 75% was needed if the former was degraded by motion artifacts) and were then transferred to a workstation (Vitrea, Toshiba Medical Systems) for processing.

2.2. Image analysis

Review of the axial images was the most important step in image analysis with thorough tracing of the vessels even if so delicate. Multiplanar reformations were used as confirmatory tool in the evaluation. The data set with the least motion artifacts was then selected as representing the optimal reconstruction window setting. The selected images were displayed using two visualization techniques, multiplanar reformation and volume rendered 3D reconstruction. Multiplanar reformation was individually adjusted to the long axis of the structure of interest to obtain accurate measurements. Volume rendering was the most lengthy postprocessing technique, yet it was helpful for the 3D visualization of complex anatomy.

Imaging data analyses were performed by one author (RZ) with six years of MDCT imaging experience in congenital heart disease, who was supervised by a second author (AAEl-B) with ten years of MDCT imaging experience. The two observers were unaware of the details of the clinical investigations.

2.3. Calculations

Six measurements were taken from the pulmonary arteries, the maximum transverse diameters of the proximal and distal segments of the main pulmonary trunk, the right main and left main pulmonary arteries at their widest dimension on the raw axial images. The diameters of the ascending and descending thoracic aorta as well as the aortic arch were also measured

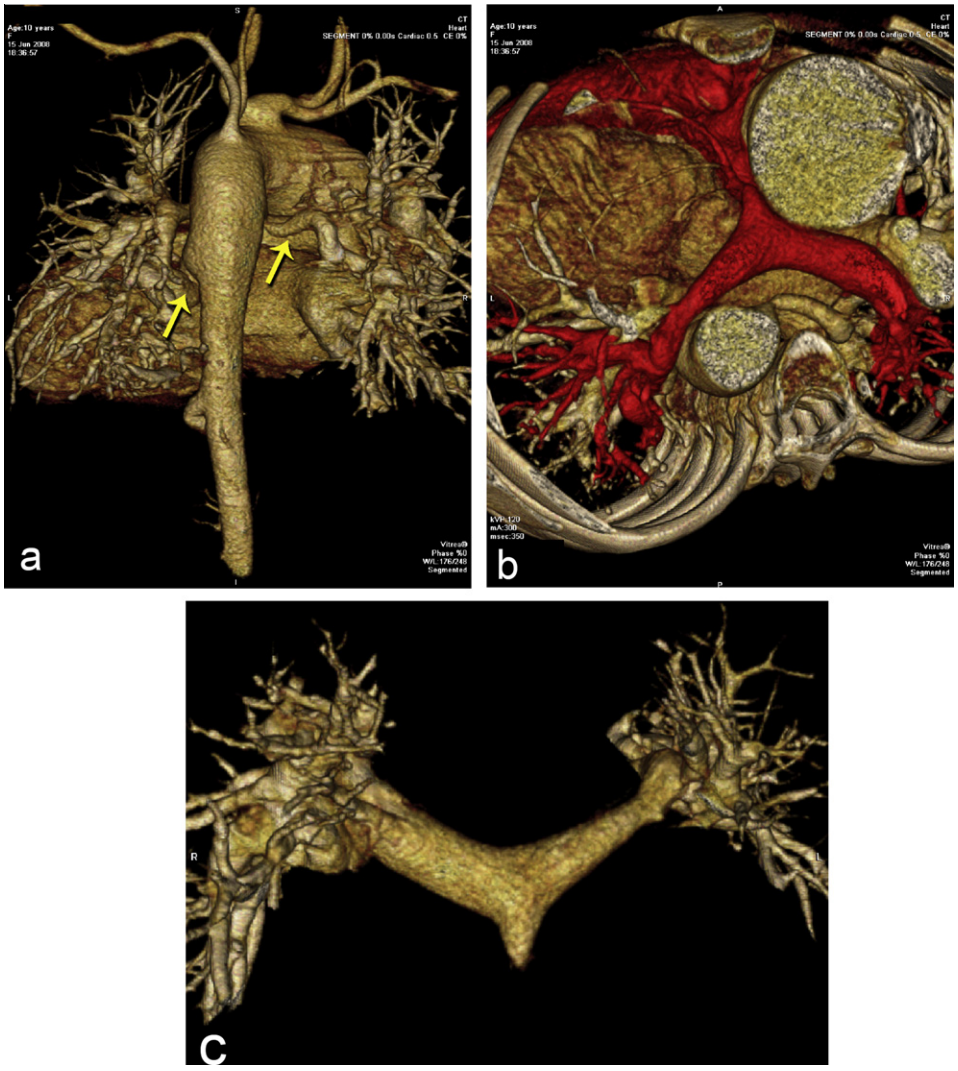

Figure 1 MDCT (64 channel) 3D VR images of a 10 years old female patient diagnosed with F4. (a) Posterior view of the heart showing bilateral MAPCA's (arrows). (b) Postero-superior view of the thorax showing atresia of the proximal segment of the main pulmonary artery with only a short segment measuring about 7 mm in diameter, relative small caliber of the left pulmonary artery and marked dilatation of the ascending thoracic aorta (4.4 cm in diameter). (c) Selectively cropped pulmonary arterial tree in antero-superior view showing the main pulmonary trunk atresia.

on the raw axial images (the descending aorta was measured at the level of the diaphragmatic crus).

CT McGoon ratio was calculated in patients with evidence of pulmonary hypoplasia or atresia according to the following equation (14):

$$x = \frac{\text{LPA} + \text{RPA}}{\text{DAo}}$$

where LPA = left pulmonary artery, RPA = right pulmonary artery and DAo = descending aorta at the level of the diaphragmatic crus. A McGoon ratio cut off value is 1.7, below which indicates a rather small caliber central pulmonary artery that may warrant more rapid surgical shunts.

The diameters of aorto-pulmonary collaterals (MAPCAs), as well as patent ductus arteriosus (PDA) were also calculated when detected in the study.

2.4. Statistical analysis

Results are expressed as means ± 1 standard deviation for normally distributed data; otherwise, medians and ranges are shown. Patient characteristics were compared between groups by using the Student *t* test. Analysis was performed by using statistical software. A *P* value of less than 0.05 was considered to indicate a statistically significant difference. No adjustments were made regarding the multiple tests performed.

3. Results

3.1. Image data reconstruction

Twenty three patients with tetralogy of Fallot were imaged with a 64 channel MDCT scanner. All patients were also imaged with concurrent echocardiography.

Selection of the optimal reconstruction window settings and the subsequent evaluation of the MDCT scans using the two visualization techniques took approximately 1 h.

3.2. Classic MSCT imaging findings of Fallot's Tetralogy

Twenty two patients had situs solitus, while only one patient had atrio-ventricular and ventriculo-arterial discordance. They all had a ventricular septal defect ($n = 23$), where one patient had an associated patent foramen ovale. Sixteen patients had mild right ventricular hypertrophy (70%), while only seven patients (30%) had severe right ventricular hypertrophy. Twenty one patients (91%) had an overriding aorta, two patients had double outlet right ventricle (9%), while only one patient had associated thickening of the aortic valve.

3.3. Common associations of Fallot's Tetralogy

All patients had complex pulmonary artery anatomy. Two cases had atresia of the main pulmonary artery trunk as well as the right and left main branches (9%) (Fig. 4), one patient had atresia of the main trunk and stenosis of the left pulmonary artery branch (4%) (Fig. 1), two had atresia of the main pulmonary artery trunk alone (9%). The rest of the patients ($n = 18$) had different degrees of pulmonary artery stenosis, namely, 17% had main trunk stenosis only ($n = 4$) ranging from 4 mm to 5 mm in diameter; 17% had main trunk and both pulmonary artery branch stenoses ($n = 4$) ranging from 1.8 mm to 7 mm in diameter; 9% had main trunk and left pulmonary artery stenosis ($n = 2$) ranging from 1.8 mm to 5 mm in diameter; 13% had left pulmonary artery branch stenosis only ($n = 3$) ranging from 2 mm to 4.8 mm in diameter; 17% had left and right pulmonary artery stenosis ($n = 4$) ranging from 1.4 mm to 9 mm in diameter and only 4% had right pulmonary artery branch stenosis only ($n = 1$).

Additionally, 10 patients (43%) had infundibular pulmonary artery stenosis (Figs. 2 and 3) (ranging from 1 mm to 7 mm in diameter), and 13 patients (57%) had aortopulmonary collateral circulation (collateral diameters ranged from 1 to 3.5 mm).

The McGoon ratio was below the cutoff value of 1.7 in seven cases (30%), while the rest of the cases yielded normal values.

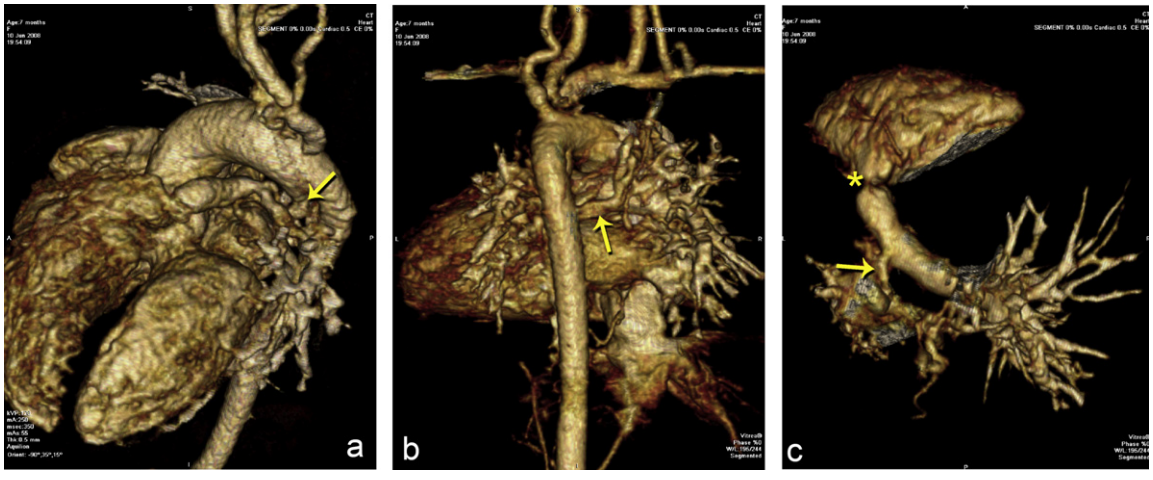

Figure 2 MDCT (64 channel) 3D volume rendered images of a 7 month old female patient diagnosed with Tetralogy of Fallot. (a) Lateral view of the heart showing a prominent PDA of about 6.7 mm in diameter is seen arising from the distal arch opposite the left subclavian artery origin. It descends in a tortuous tapering course towards the postero superior aspect of MPA, joining it at the site of LPA origin. (b) Posterior view of the heart showing right sided aorta-pulmonary collaterals (arrows). (c) Selectively cropped VR image of the pulmonary arterial system in postero-superior view showing pulmonary infundibular stenosis (∗) and stenotic LPA origin (arrow).

Seven cases (30%) had associated right sided aortic arch, while three cases (13%) had associated ASD. Only one case (4%) showed an abnormal origin of the left anterior descending coronary artery branch (LAD).

Eleven patients had an associated patent ductus arteriosus (PDA) that extended anteriorly from the anterior border of the descending aorta to the superior aspect of the main pulmonary artery, 10 of which were adjacent to the left pulmonary artery bifurcation (Figs. 2 and 4), while only one was adjacent to the right pulmonary artery. All these ducts except one were patent, and only one case showed that the duct was closed. Using multiplanar reformations of the true and oblique axial, sagittal, and coronal section data, we measured the widest diameter of the ducts (mean 4.7 mm ± 2 mm).

Two cases with main pulmonary artery atresia were associated with MAPCA, one had a single right sided collateral, while the other had a single right sided major collateral and two left sided major collaterals (Figs. 1 and 3). Two other cases with pulmonary artery stenosis were associated with MAPCAs, each had two collaterals on the right side and two collaterals on the left side.

3.4. Uncommon associations of Fallot's Tetralogy

Two cases (9%) were associated with dilatation of the ascending thoracic aortic segment, measuring about 4.4 mm (Fig. 1b) and 4 mm, respectively. Five cases (22%) were also associated with relative stenosis of the descending thoracic aorta, having a maximum diameter of 0.5 mm each (Fig. 4).

Abnormal origins of the thoracic aortic branches were associated with some of the cases, namely: five cases (22%) showed a common brachio-cephalic trunk (Fig. 1), three cases (13%) showed the right subclavian artery and the right common carotid artery originating from the aortic arch, one case (4%) was associated with an aberrant left subclavian artery, while two others (9%) were associated with retrooesophageal left

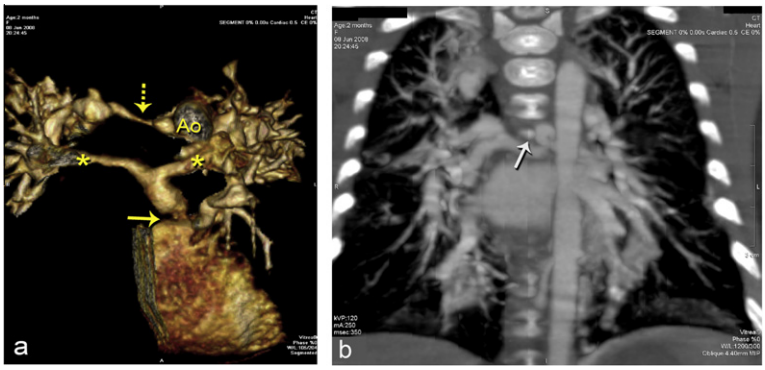

Figure 3 MDCT (64 channel) 3D volume rendered images of a 2 month old female patient diagnosed with Tetralogy of Fallot. (a) Antero-superior view of the heart showing pulmonary infundibular stenosis (arrow), small sized main pulmonary arterial branches (∗) and prominent MAPCA (dotted arrow). Ao = aorta. (b) Coronal MIP image of the chest showing prominent right sided MAPCA (arrow).

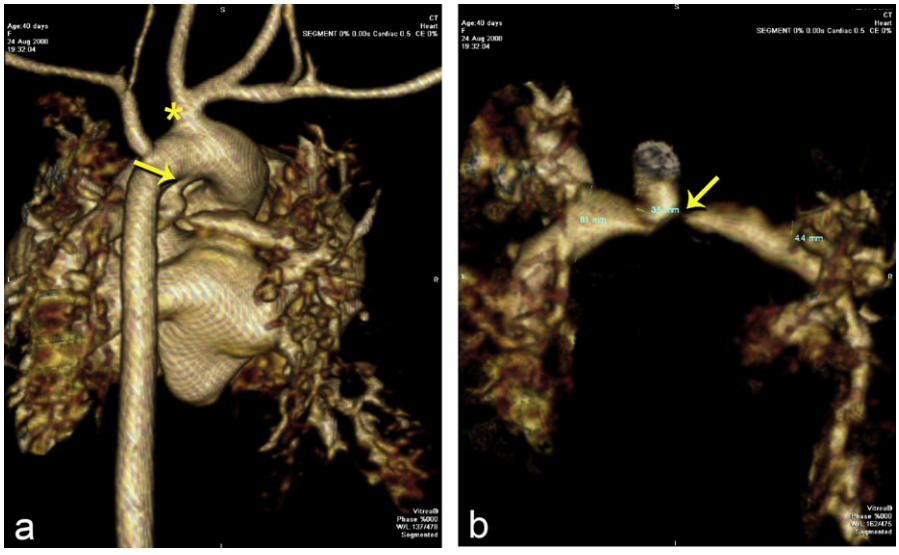

Figure 4 MDCT (64 channel) 3D volume rendered images of a 40 day old female patient diagnosed with Tetralogy of Fallot. (a) Posterior view of the heart showing a prominent PDA. Common origin of the left common carotid artery and the innominate trunk via common trunk off the aorta is also noted also (∗). (b) Selectively cropped image of the pulmonary arterial tree in posterior view showing significant proximal right pulmonary artery stenosis at its origin (arrow);at PDA junction (∗).

subclavian arteries and the left vertebral arteries originated from the arch separately.

Seven cases (30%) showed prominent pulmonary veins, in one case the veins appeared to be attenuated (Fig. 3), while in one case there was associated partial anomalous pulmonary venous drainage.

One of the cases had associated bilateral superior vena cava, an azygos vein and the hepatic veins were seen to drain into the right atrium.

One of the cases associated with an ASD showed bilateral SVC, while another one was also associated with a retro-aortic course of the left innominate vein.

One case was associated with double infrahepatic inferior vena cava (IVC).

4. Discussion

Congenital heart disease can be diagnosed by a large number of imaging modalities. Echocardiography is still the preferred modality for imaging intracardiac anatomy and hemodynamics. However, it has some limitations, namely the small field of view, the variable acoustic window, its inability to penetrate air and bone and the associated difficulty in assessing the extracardiac vascular structures (10).

Cardiac angiography is an invasive modality that illustrates significant hemodynamic data and undoubtedly demonstrates the accessible vascular anatomy. However, it is often limited in diagnosing venous connections and arterial anatomy distal to high-grade stenosis or atresia. It also uses high doses of ionizing radiation and is limited by the risks attributed to iodinated contrast material (10).

MDCT is a relatively new technology, which can be done safely and quickly even in small infants. It clearly demonstrates information about the great vessels and coronary arteries and can non-invasively diagnose the complex cardiac anatomy in these patients (15). It provides superior diagnostic accuracy in assessment of patients with tetralogy of Fallot regarding the central and peripheral pulmonary arteries, aorto-pulmonary collateral vessels as well as in demarcation of the abnormal venous anatomy and veno-atrial connections (10).

In the current study all the cardiac and extracardiac associations were clearly diagnosed, even those that were missed or were unattainable during the echocardiographic examination.

The complex pulmonary artery anatomy and pulmonary atresia in patients with tetralogy of Fallot is easily defined by MDCT, along with the major aorto-pulmonary collateral vessels (16,17). Pulmonary atresia is the most severe form of antero-cephalad deviation of the outlet septum. However, in some occasions the pulmonary valve is affected solely by being completely imperforate, not just stenotic (3). In the current study, MDCT diagnosed two cases (9%) of pulmonary atresia involving the main trunk as well as the major branches, one case (4%) with main trunk and left pulmonary artery atresia and two cases (9%) with pulmonary artery trunk alone. The rest of the cases (78%) were diagnosed by MDCT with different degrees of pulmonary artery stenosis. No cases with pulmonary vascular abnormality were missed by this modality.

In patients with tetralogy-type pulmonary atresia, a diversity of systemic sources share in the pulmonary blood flow (18). In about 50% of patients with pulmonary atresia, there is confluence of the right and left pulmonary arteries, with persistently patent arterial duct giving blood to the pulmonary arteries (19). Eleven patients (48%) were diagnosed with PDA in the current study, and MDCT could clearly demonstrate their patency, their extensions, their length and diameter as well as their exact location.

In the other half of these patients, there is multifocal pulmonary arterial supply (3). In patients who obtain some or all of their pulmonary blood supply through vessels from the aorta or other splanchnic arteries, the coronary arteries supply blood in about 10% of cases. Very rarely, the coronary artery may be connected to the pulmonary artery, thereby serving as a major or sole source of flow (18). However, none of the cases in the current study were supplied by the coronary arteries.

In cases with atretic or markedly hypoplastic pulmonary arteries, multiple collateral arteries give the blood supply to the lungs, or a combination of collateral arteries and an arterial duct are the source (3).

In some rare cases of Fallot's Tetralogy there is associated situs inversus. The assessment of sidedness in general (situs) should include cardiac, pulmonary, and abdominal sidedness, which are usually concordant. Cardiac sidedness is identified by the position of the morphologic right atrium and is different from cardiac position, cardiac orientation, and the positions of the ventricles or great arteries. In situs solitus (the normal configuration), the morphologic right atrium lies to the right of the morphologic left atrium. In situs inversus, the morphologic right atrium lies to the left of the morphologic left atrium (13). All the cases of this study had situs solitus, except for one case which had atrioventricular and ventriculoarterial discordance.

In cases with overriding of the aorta, the aorta becomes more inclined to the right ventricle than to the left ventricle, leading in many cases to the ventriculo-arterial connection of double outlet right ventricle (3). In patients where the aorta originates mainly from the right ventricle there is a greater risk of developing obstruction of the left ventricular outflow tract. This tract is produced by a patch which closes the ventricular septal defect connecting the left ventricle to the aorta. In these cases, this patch is markedly longer than that seen when the aorta arises mostly from the left ventricle (3). Two cases in this study showed double outlet right ventricle, one was also associated with a right sided aortic arch.

Two percent of patients with tetralogy of Fallot have an associated atrioventricular septal defect (3). However, in the current work, three cases (13%) had an associated ASD, which was significantly more than that reported in the literature. The presentation and initial medical management of Tetralogy of Fallot patients with this association remain unchanged, however surgical repair and post-operative care are more complex (3).

Billiart et al., reported that 25% of patients with tetralogy of Fallot have an associated right aortic arch, which causes no haemodynamic consequence. This was more or less in concordance with our study results which showed seven cases (30%) having this association.

4.1. Limitations

Easy availability, short scanning times and non-invasive vascular imaging are some of the advantages of MDCT. Accurate extracardiac arterial and venous vascular imaging is attainable by contrast-enhanced MDCT. However there are still

drawbacks of MDCT including patient exposure to ionizing radiation and the risks of iodinated contrast material (10).

Meticulous stress must be put on radiation exposure issues, because the first CT examination in patients with tetralogy of Fallot usually occurs in childhood or in early adulthood, and more often than not repeat scanning is essential. ECG-gated MDCT exposes the patient to a higher risk of radiation, so the benefits of evaluating the ventricular function, cardiac valves, small intracardiac abnormalities, and coronary arteries must prevail over these risks. The effective radiation dose from ECG-gated CT of the heart is estimated to be approximately 15 mSv. For comparison, the effective radiation dose from nongated CT of the chest is approximately 5 mSv (13). We used ECG-controlled tube current modulation (ECG pulsing) technique for our young patients to reduce the amount of radiation exposure of these patients. However, patients with a heart rate >200 beats/min could not benefit from this technique and hence used the same technical parameters used in normal MDCT cases.

The second issue of contrast enhancement risks was partially resolved in the current study by the use of non-ionic contrast agent calculated according to the patient weight, with a maximum dose of 2 ml/kg, injected at 2 ml/s, thus reducing the risks of use of iodinated contrast material and the higher doses needed.

5. Conclusion

MDCT examinations are most fruitful when specific diagnostic questions are asked by the cardiologists, surgeons, and radiologists after careful assessment of the clinical condition and other imaging findings. This customized approach improves the diagnostic accuracy and reduces unneeded prolongation of the study and sedation times. A careful preoperative perceptive of the complex cardiovascular anatomy in patients with Tetralogy of Fallot aids in exposing the patient to a directed and prepared surgical approach.

References

(1) Fallot ELA. Contribution a l'anatomie pathologique de la maladie bleu (cyanose cardiaque). Marseille Med 1888; 77–93.

(2) Becker AE, Connor M, Anderson RH Tetralogy of Fallot: a morphometric and geometric study. Am J Cardiol 1975;35:402–12.

(3) Bailliard F, Anderson RH Tetralogy of Fallot. Orphanet J Rare Dis 2009;4:2.

(4) Ferguson EC, Krishnamurthy R, Oldham SAA Classic imaging signs of congenital cardiovascular abnormalities. RadioGraphics 2007;27:1323–34.

(5) Boechat MI, Ratib O, Williams PL, et al. Cardiac MR imaging and MR angiography for assessment of complex tetralogy of Fallot and pulmonary atresia. RadioGraphics 2005;25:1535–46.

(6) Dabizzi RP, Teodori G, Barletta GA, et al. Associated coronary and cardiac anomalies in the tetralogy of Fallot: an angiographic study. Eur Heart J 1990;11:692–704.

(7) Brickner ME, Hillis LD, Lange RA Congenital heart disease in adults – second of two parts. NEJM 2000;342(5):334–42.

(8) Groh MA, Meliones JN, Bove EL, et al. Repair of tetralogy of Fallot in infancy: effect of pulmonary artery size on outcome. Circulation 1991;84(Suppl. 5):III 206–212.

(9) Touati GD, Vouhe PR, Amodeo A, et al. Primary repair of tetralogy of Fallot in infancy. J Thorac Cardiovasc Surg 1990;99:396–402.

(10) Haramati LB, Glickstein JS, Issenberg HJ, et al. MR imaging and CT of vascular anomalies and connections in patients with congenital heart disease: significance in surgical planning. RadioGraphics 2002;22:337–49.

(11) Flohr T, Stierstorfer K, Raupach R, et al. Performance evaluation of a 64-slice CT system with z-flying focal spot. Rofo 2004;176:1803–10.

(12) Manghat NE, Morgan-Hughes GJ, Marshall AJ, et al. Multidetector row computed tomography: imaging congenital coronary artery anomalies in adults. Heart 2005;91:1515–22.

(13) Leschka S, Oechslin E, Husmann L, et al. Pre- and postoperative evaluation of congenital heart disease in children and adults with 64-section CT. RadioGraphics 2007;27:829–46.

(14) Chen Bang-Bin, Chen Shyh-Jye, Wu Mei-Hwan, Li Yiu-Wah, Lue Hung-Chi EBCT – McGoon ratio. A reliable and useful method to predict pulmonary blood flow non-invasively. Chin J Radiol 2007;32:1–8.

(15) Khositseth A, Pornkul R, Siripornpitak S Diagnosis of tetralogy of Fallot with anatomically corrected malposition of the great arteries and single coronary artery by multidetector CT. Br J Radiol 2006;79:e5–7.

(16) Westra SJ, Hill JA, Alegjos JC, Galindo A, Boechat MI, Laks H Three-dimensional helical CT of pulmonary arteries in infants and children with congenital heart disease. AJR Am J Roentgenol 1999;173:109–15.

(17) Luciani GB, Wells WJ, Khong A, Starnes VA The clamshell incision for bilateral pulmonary artery reconstruction in tetralogy of Fallot with pulmonary atresia. J Thorac Cardiovasc Surg 1997;113:443–52.

(18) Mawson JB Congenital heart defects and coronary anatomy. Tex Heart Inst J 2002;29(4):279–89.

(19) Tetralogy of Fallot and Pulmonary Atresia. Pediheart Website <http://www.pediheart.org/practitioners/defects/ventriculoarterial/TOF_PA.htm>. Published February 14, 2004. [accessed 20.03.10].